Role of Austenitization and Pre-Deformation on the Kinetics of the Isothermal Bainitic Transformation

H.-G. LAMBERS, S. TSCHUMAK, H.J. MAIER, and D. CANADINC

The role of time-temperature path on the isothermal austenite-to-bainite phase transformation of low alloy 51 CrV 4 steel was investigated and the corresponding microstructures were analyzed. The important finding is that an incomplete initial austenitization treatment leaves undissolved carbides in the matrix, such that lower carbon and chromium content in the matrix result, eventually accelerating the phase transformation. Furthermore, the residual carbides constitute additional nucleation sites for the bainite plates, speeding up the process even further. Also, both plastic pre-deformation of the supercooled austenite and application of external elastic stresses during the phase transformation lead to transformation plasticity by enhancing the stress fields, providing a driving force for the growth of bainite plates along a preferred orientation. Overall, the current results constitute the first step toward establishing a database for constructing a realistic microstructure-based model for simulating metal forming operations involving austenite-to-bainite phase transformation.

DOI: 10.1007/s11661-009-9827-z

I. INTRODUCTION

STEEL is generally the material of choice when it comes to structural components that demand high strength and good ductility. Furthermore, properties of steels can be tailored by varying the process parameters, such as deformation stresses and strains, and temperature. In particular, temperature is one key parameter affecting the final microstructure, such that the mechanical properties of a steel strongly depend on the temperature-time path during processing.[1] Moreover, the degree of anisotropy is dictated by temperature, such that an anisotropic microstructure is induced on an initially isotropic one by an increasing temperature gradient during cooling. For instance, forging is mostly expected to lead to an anisotropic microstructure as variations in the local temperature-time-deformation paths accompanied by inhomogeneously dissolved carbide bands can lead to dimensional instability,[2] resulting in high postprocessing costs. However, the anisotropic microstructure evolution during forging may also be used to advantage, such that a functionally graded workpiece could be manufactured.[3]

Producing a near-net-shape workpiece during forging would prevent additional costs since minor post processing, such as turning or milling, is needed. A near-net-shape workpiece should not only guarantee the geometrical stability, but it is also expected to fulfil the required mechanical properties within the workpiece. Ideally, the chosen temperature-deformation-time path should allow for different microstructures within one workpiece, since the desired properties might vary with the location within the final workpiece.[3,4] Especially for products, such as gears, which are hard at the surface and tenacious in the inner part, one has to optimize the forging process. However, this requires a solid knowledge of factors dictating the geometrical stability, such as phase transformations, which are accompanied by volumetric changes that lead to distortion. In many cases, distortion can be minimized by reducing the temperature gradients and the resulting stresses, yet even small elastic stresses and temperature gradients can affect the phase transformation kinetics and the local microstructure.[5–7] It is well known that elastic stresses are capable of accelerating the phase transformation kinetics,[6,8,9] which has recently come into consideration in the prediction of the final microstructure of forged steel products.[10,11]

Several models were forwarded,[12–17] which successfully explain the occurrence of transformation plasticity, *i.e.*, the inhomogeneous portion of the plastic strain accompanying the phase transformation when stress is superimposed during transformation. However, these models are not suitable when the superimposed stresses are beyond the elastic regime or other phenomena such as creep, come into the picture.[18–20] For instance, during forging large plastic strains and temperature gradients are commonly observed and their magnitudes depend on the particular location within the workpiece. Thus, thorough experimental programs have been undertaken with the aim of identifying the locally observed phenomena, relating various stress-strain states and local temperatures to the phase transformation kinetics.[21–23] Specifically, the effects of plastic pre-deformations and elastic stresses on the kinetics of isothermal bainitic transformations were monitored in

H.-G. LAMBERS and S. TSCHUMAK, Research Assistants, and H.J. MAIER, Professor, are with Lehrstuhl für Werkstoffkunde (Materials Science), University of Paderborn, 33095 Paderborn, Germany. Contact e-mail: hmaier@mail.uni-paderborn.de D. CANADINC, Assistant Professor, is with the Department of Mechanical Engineering, Koc University, 34450 Istanbul, Turkey.

Manuscript submitted August 27, 2008.
Article published online April 8, 2009

stable and supercooled austenitic microstructures.[21–25] It was demonstrated that plastic pre-deformations larger than 10 pct in compression tend to retard the phase transformation kinetics due to the stabilization of austenite,[24] or accelerate the phase transformation along with the superimposed elastic stresses.[8,26] Furthermore, transformation plasticity and anisotropic shape change were prevalent during the phase transformation.

Two widely-accepted approaches are used to explain the concept of transformation plasticity: the Magee approach[27] and the Greenwood–Johnson approach.[28] According to the Magee model, which was initially developed for martensitic reactions and later adopted for bainitic transformations, the transformation plasticity stems from the alignment of martensitic or bainitic variants when stress is superimposed during transformation.[27,29,30] The additional mechanical driving force helps to form variants having a preferred alignment with respect to the loading axis at the expense of other variants. As a result, the final microstructure is anisotropic and brings about anisotropic transformation strains. Considering the shape change occurring during bainitic and martensitic transformations in a displacive manner, it was shown that the macroscopic shape change can be linked to a preferred alignment of variants, such that the number of variants favored is dictated by the superimposed stresses.[29]

The Greenwood–Johnson model, on the other hand, postulates that the transformation plasticity strains originate from microdeformations of the weaker phase since there is a volume difference between the parent and the product phases. When the phase transformation is superimposed by an elastic stress the product phase grows at the expense of the parent phase toward a certain direction, yielding transformation strains.[23,28] As opposed to the Magee model, in the Greenwood–Johnson approach it is assumed that the resulting transformation plasticity strains formed during transformation do not vanish during a reaustenitization.[12] It was demonstrated that in the case of repeated heating and cooling of a 16MND5 steel, the transformation-induced plasticity strain is not altered by bainitic transformations but indeed accumulates with each cycle,[19,23] which favors the Greenwood–Johnson mechanism. Nevertheless, both mechanisms can be simultaneously active during phase transformation where the relative effectiveness of each mechanism is governed by transformation parameters, such as transformation temperature.[19,23]

When transformation plasticity is present, based on the principles of the Greenwood–Johnson mechanism no preferred alignment of the bainitic microstructure would be visible. Thus, an investigation of the final microstructure can help decide whether the Greenwood–Johnson or the Magee mechanism facilitates the transformation plasticity, which constitutes one motivation of the current work. Specifically, the microstructures of pre-deformed samples that exhibited transformation plasticity during phase transformation and those that transformed in the absence of any superimposed stresses were monitored through electron backscatter diffraction (EBSD). The key finding is that variant selection took place during deformation prior to the phase transformation, indicating that the resulting transformation plasticity followed the Magee mechanism.

In many of the previous investigations the samples were fully austenitized prior to the subsequent phase transformation, where the austenitization time was held constant.[20,24,25,31–33] However, during forging the heating and cooling rates can be extremely high, which necessitates the availability of transformation kinetics data for various temperature-time paths. In order to shed light on the effect of austenitization temperature and time on the isothermal phase transformation kinetics, two different heat treatments were considered in the current work: a conventional heat treatment based on available time-temperature-transformation diagrams[1] and one derived from an actual forging process.[21] As a result, it was demonstrated that the different temperature-time paths have a significant influence on the isothermal bainitic phase transformation kinetics. For instance, the time to fully complete an isothermal bainitic transformation at 340 °C under zero stress could be more than doubled by only increasing the austenitization temperature and decreasing the austenitization time. Furthermore, it was clearly shown that plastic pre-deformations, or stresses superimposed during phase transformation, strongly affect the transformation behavior, dictating the local microstructure evolution. Overall, the current findings constitute an essential set of data that would serve as the basis for a realistic modeling effort of the forging process considered.

II. EXPERIMENTAL

The material used in this study was low alloy 51 CrV 4 steel with only minor sample-to-sample variations in the chemical composition (Table I), which assures good repeatability of the phase transformation behavior. Precisely machined thin-walled hollow specimens with an outer diameter of 10 mm were used, which had a wall thickness of only 1 mm within the gage length such that the electrical resistance of the specimens, and thus the corresponding heat conduction throughout the gage sections, was homogeneous. As a result, the samples could be heated up within seconds by resistance heating and only a negligible temperature gradient was present along the axial and radial directions. Resistance heating

Table I. Chemical Composition of the Material Studied*

Element	C	Cr	Mn	S	Pb	Si	Cu
Wt pct	0.48	0.88	0.72	0.018	0.004	0.26	0.17
	0.48	0.94	0.77	0.021	0.010	0.30	0.19

Element	Al	Ni	Mo	Nb	Ti	P	Fe
Wt pct	0.007	0.09	0.02	0.001	0.011	0.017	balance
	0.009	0.10	0.02	0.002	0.014	0.021	balance

*The data shown represent minimum and maximum values obtained from various samples.

in combination with nozzles for gas quenching also allowed for small temperature gradients during cooling due to the homogeneous air flow. The custom-built test rig used in the experiments also included a screw-driven testing machine with both an axial and a diametral extensometer.[20]

During forging, both the temperature and the stress fields are inhomogeneous, such that both the temperature and the stress states change drastically within a few seconds at the final stages of the process. The outer surface of the forged product cools down much faster than the inner part, yielding a significant temperature gradient. Furthermore, enhanced plastic strains are prevalent inside the forged product, whereas the outer surface bears smaller strains.[34] Consequently, the effect of variations in temperature, and stress and strain fields were considered separately in the current experimental scheme, in order to clearly lay out the role of each variable by avoiding the complications brought about by the simultaneous changes in all three.

In order to monitor the effect of temperature evolution on the isothermal phase transformation kinetics two different temperature-time paths were considered (Figure 1). For the first set of experiments the specimens were austenitized in accord with the conventional heat treatment at 880 °C for 5 minutes (heated up within 2 minutes), and then quenched with pressurized gas down to a temperature of 340 °C[1] with a nominal cooling rate of 45 °C/s. The chosen cooling rate was fast enough to avoid any transformation before reaching the isothermal holding temperature. The temperature was controlled using a two-color pyrometer with a short response time. An additional thermocouple was fixed inside the hollow specimens in order to ensure the stability of steady-state temperatures during austenitization, and the isothermal holding at 340 °C. For the second set of experiments, the specimens were austenitized at 1050 °C for 10 seconds (heated up within 15 seconds). This treatment was chosen because of the good comparability with the temperature evolution of one specific volume element of the considered forging process of a shaft.[21] In order to monitor the influence of different stress states on the isothermal phase transformation kinetics, the specimens were either plastically deformed prior to the phase transformation, or elastic stresses lower than the yield stress of the supercooled austenite were superimposed during the phase transformation. The pre-deformed specimens were either in a supercooled or a stable austenitic state. Pre-straining of the supercooled austenite was carried out directly after reaching the isothermal temperature of 340 °C and at a nominal strain rate of 0.02 s^{-1}. Thus, the subsequent phase transformation itself was not superimposed by the application of stress.

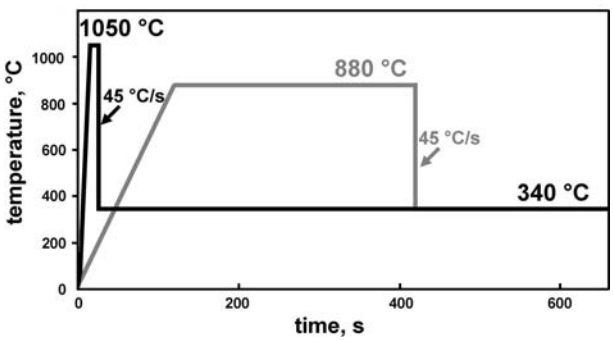

Fig. 1—Temperature-time paths employed for the two types of experiments carried out in this study.

The plastic pre-straining of the stable austenite, on the other hand, was carried out at the end of the isothermal holding at the austenitization temperature of 880 °C or 1050 °C. The samples were then unloaded shortly before the cooling started, such that the phase transformation itself took place without any superimposed external stresses. The axial and diametral strains were continuously monitored during the entire process, yet the maximum achievable axial pre-strain was 10 pct due to the ±5 pct measurement limit of the diametral extensometer. Since the austenite-to-bainite transformation is accompanied by a volumetric change, the measured strain values could be used to determine the relative volume change according to Eq. [1], as explained in the Appendix. In order to make sure that no strains due to pre-straining or due to the superimposition of elastic strains falsify the resulting values, the axial as well as the diametral strain values were set to zero, (1) directly after unloading when pre-strains were applied or (2) when the given stress level superimposed during the phase transformation was reached. In addition, the volume fractions of bainite as well as the transformation plasticity values were determined following Eqs. [2] and [3] in the Appendix.

Microhardness measurements (HV 0.1) through the wall thickness were employed to detect any decarburization. Since the wall thickness was only 1 mm, the sample was cut at a 5-deg angle to enlarge the effective measurement length.

For monitoring the effect of plastic pre-straining on the microstructure, EBSD measurements were performed on the gage sections of the hollow specimens employing a scanning electron microscope operating at a nominal voltage of 20 kV. The surfaces of the EBSD samples were prepared by conventional polishing followed by electropolishing using a 5 pct perchloric acid solution. A light optical microscope was deployed for determining the initial austenite grain size depending on the austenitization temperature. For this measurement the specimens were etched using a solution containing aqueous picric acid and 0.1 pct hydrochloric acid. The average austenite grain size depending on the austenitizing treatment was then determined following the German standard DIN EN ISO 643.

Transmission electron microscopy (TEM) analysis was conducted to decide whether the different austenitization treatments were complete or not. For the TEM analysis, thin slices were cut out of the thin-walled hollow specimens and then ground to 150 μm. Conventional twin-jet electropolishing using a 5 pct perchloric acid solution under an applied potential of 25 V at –40 °C was used to achieve electron transparency, and the TEM employed was operated at a nominal acceleration voltage of 200 kV.

III. RESULTS

As demonstrated in Figure 2, the austenitization treatment has a pronounced influence on the subsequent phase transformation kinetics. The isothermal phase transformation at 340 °C is delayed when the initial austenitization takes place at 1050 °C only for 10 seconds instead of being carried out for 5 minutes at 880 °C. There are several reasons that can cause such a significant change in the transformation behavior such as nitrogen hardening, decarburization, a change in initial austenite grain size, or residual carbides not dissolved during the austenitizing treatment. Whereas the time-temperature path used for the austenitization treatment significantly affects the transformation kinetics, it is clear from Figure 2 that there is no effect whether nitrogen gas or inert argon is used as the environmental medium.

In Figure 3 the initial austenite grain sizes of a specimen austenitized at 1050 °C for 10 seconds and of another sample austenitized at 880 °C for 5 minutes are revealed and no significant difference in grain size is apparent between the two cases. The average austenite grain size for both cases was determined as 16 μm, corresponding to G9 in the ASTM standard.

Figure 4 presents the hardness values along the wall thickness of a specimen completely transformed to bainite at 340 °C following austenitizing at 880 °C for 5 minutes. Obviously the hardness values are almost constant except for a thin surface layer with a thickness of approximately 0.1 mm. The linear increase in hardness from 400 HV0.1 at the surface to an almost constant saturation value of 500 HV0.1 at a depth of 0.1 mm is due to decarburization, and spectroscopic analysis showed that the average carbon content in this layer is reduced from the bulk value of 0.48 to 0.42 wt pct. The spectroscopic device employed allowed for a carbon content measurement with an accuracy of ±0.01 wt pct. By contrast, the sample austenitized at 1050 °C for 10 seconds after a complete bainitic transformation at 340 °C showed no effect of decarburization and displayed constant hardness values throughout the samples wall thickness (Figure 4).

Since the decarburized layer is rather small as compared to the wall thickness of the specimens, the reduced carbon content of the samples austenitized at 880 °C for 5 minutes should only have a minor effect on the kinetics of the subsequent bainitic phase transformation at 340 °C. Even if one assumes that the average carbon content in the complete specimen and not only in the surface layer was reduced to 0.42 wt pct,

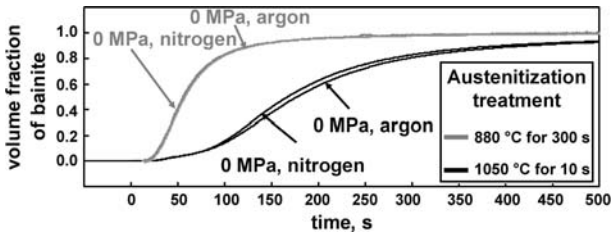

Fig. 2—Influence of austenitization treatment and environmental media on the isothermal bainitic phase transformation kinetics at 340 °C in the absence of superimposed stresses.

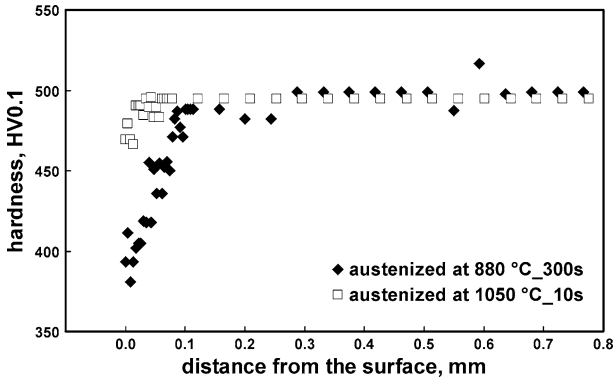

Fig. 4—Hardness measurements through the wall thickness of specimens austenitized at 880 °C for 5 min and at 1050 °C for 10 s.

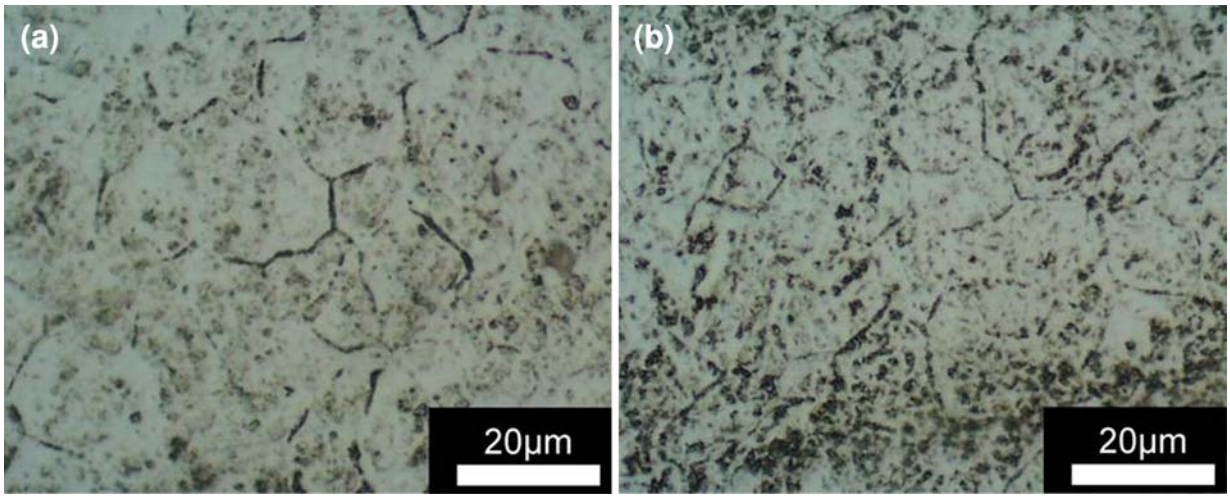

Fig. 3—Optical micrographs showing the initial austenite grain size after austenitization at (*a*) 1050 °C for 10 s and (*b*) at 880 °C for 5 min.

a simulation with JMatPro software using the chemical composition as well as the initial austenite grain size and austenitization temperature as input parameters revealed that there is almost no change in transformation characteristics. Thus, decarburization effects are considered to be negligible in the present case.

The TEM studies were performed to verify whether the austenitizing treatment was suitable to dissolve the carbon homogeneously in the matrix. Residual carbides due to an incomplete austenitization reduce the content of carbon and alloying elements (basically chromium) in the matrix. Since the bainitic reaction is accompanied both by diffusive and displacive transformation mechanisms, carbides are always present in the transformed samples. Thus, residual carbides can only be distinguished easily from those formed during the bainitic reaction if the two types differ drastically in size or location within the matrix. Therefore, an additional test with a specimen martensitically transformed following an austenitization at 880 °C for 5 minutes was conducted. Since the martensitic reaction is not accompanied by diffusive mechanisms, any carbides obtained in the final microstructure must be due to an incomplete dissolution mechanism. Figure 5(a) presents a TEM image obtained from a specimen isothermally transformed at 340 °C to bainite after an austenitization at 880 °C for 5 minutes, and Figure 5(b) shows a TEM image obtained from a martensitically transformed specimen following the same austenitizing treatment. Energy dispersive spectroscopy (EDS) conducted on the TEM foils revealed that the dark hardly electron transparent areas are large residual carbides with an average chromium content about 8 times the nominal bulk value. By contrast, no such areas were detected in samples austenitized at 1050 °C for 10 seconds, and the carbides visible in Figure 5(c) were formed during the bainitic reaction.

Fixing the temperature-time path simplifies comparison between the phase transformation behaviors under different stress states. However, during forging the temperature-time path varies with the position in the product. Thus, modeling the forging process requires detailed information on the effect of evolution and distribution of temperature on the kinetics of the phase transformation. Therefore, the two temperature-time paths of 880 °C–5 minutes, and 1050 °C–10 seconds were chosen to account for the role of both incomplete and complete austenitization treatments, and an incomplete austenitization was demonstrated to accelerate the phase transformation (Figure 2). However, there are other parameters, such as the external stresses superimposed during phase transformation or plastic pre-deformation that may also dictate the transformation kinetics. Therefore, the scope of experiments was broadened to observe the role of different stress states on the two temperature-time paths selected, such that the specimens were either plastically deformed in a stable or a supercooled austenitic state or a stress lower than the yield stress of the supercooled austenite was applied during the subsequent phase transformation.

Changes in stress distribution have a noticeable impact on the kinetics of the isothermal bainitic phase transformation, such that both the plastic pre-deformation of the supercooled austenite and the presence of elastic stresses accelerate the isothermal phase transformation following both austenitization treatments at 880 °C for 5 minutes and 1050 °C for 10 seconds (Figures 6 and 7). In the current work only small plastic strains of 5.5 pct or smaller were considered due to the fast transformation rate of the steel. Plastic deformations beyond 5.5 pct strain brought about a pronounced increase in temperatures indicating that the phase transformation started to settle in already during the pre-deformation stage. The accelerating affect of the small plastic pre-deformations is evident from the experimental results, such that the transformations start earlier following a 5.5 pct plastic pre-deformation (Figures 6 and 7). At the strain rate used, if the plastic pre-deformation exceeds 5.5 pct strain, the time necessary for the pre-straining increases concomitant with the

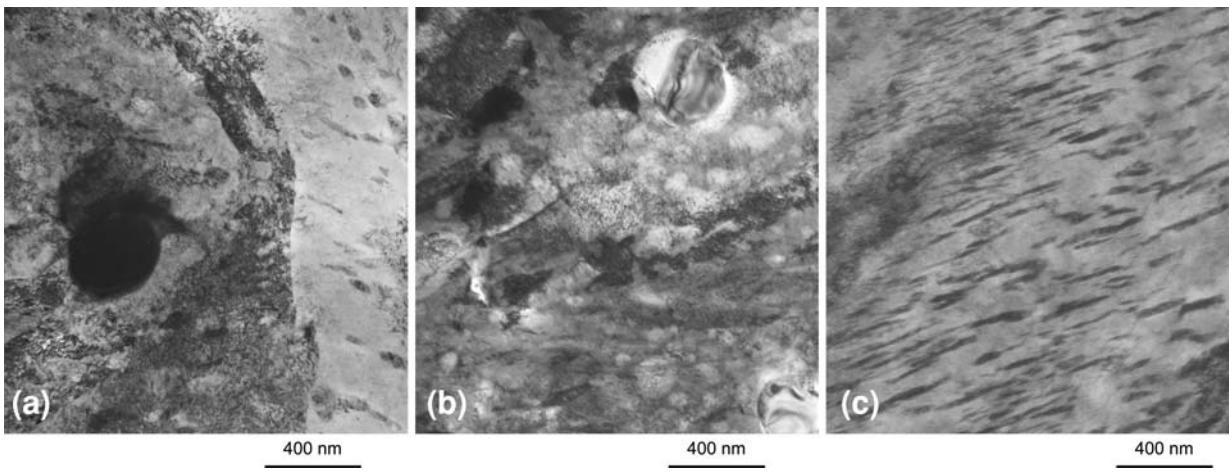

Fig. 5—TEM micrographs showing the microstructure of (*a*) specimen transformed isothermally at 340 °C to bainite following an austenitization at 880 °C for 5 min, (*b*) specimen transformed martensitically following an austenitization at 880 °C for 5 min, and (*c*) specimen transformed isothermally at 340 °C to bainite following an austenitization at 1050 °C for 10 s.

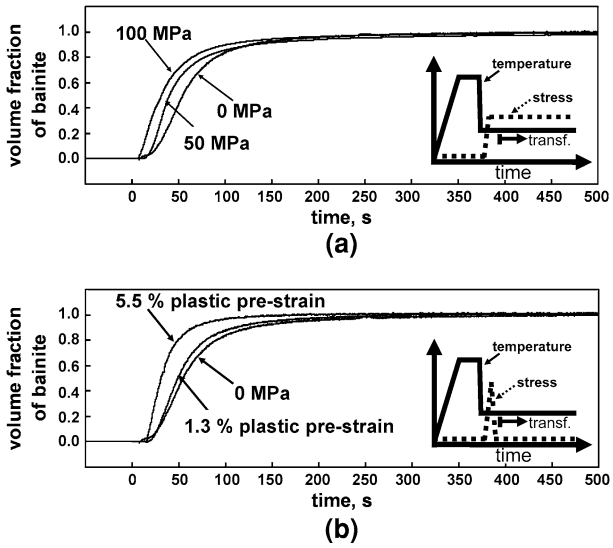

Fig. 6—Isothermal phase transformation at 340 °C in samples austenitized at 880 °C for 5 min: (*a*) effect of uniaxial external elastic stress and (*b*) effect of uniaxial external pre-strain. Plastic pre-strains were applied at 340 °C and samples were unloaded before the onset of the phase transformation.

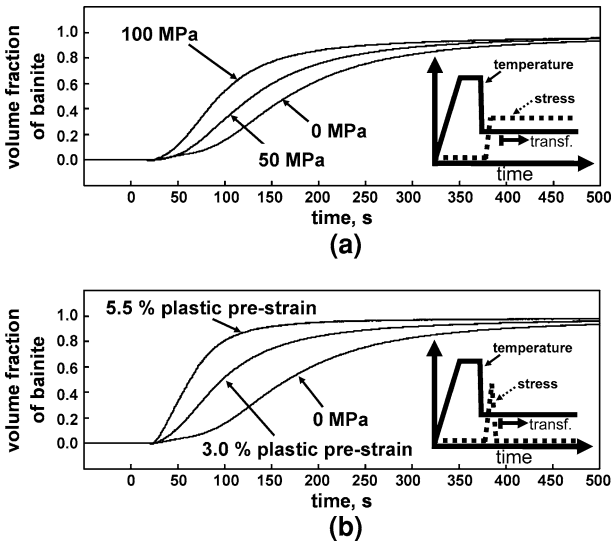

Fig. 7—Isothermal phase transformation at 340 °C in samples austenitized at 1050 °C for 10 s: (*a*) effect of uniaxial external elastic stress and (*b*) effect of uniaxial external pre-strain. Plastic pre-strains were applied at 340 °C and samples were unloaded before the onset of the phase transformation.

increasing plastic strain, leaving less time for the unloading, such that a complete unloading was no longer possible prior to the phase transformation. Thus, to ensure comparability between different sets of experiments the strain rate was fixed and no experiments were performed where the samples were more heavily deformed in the supercooled austenitic state.

However, pre-strains up to 10 pct were achievable under tensile loading at the austenitization temperature (Figure 8). Neither a 10 pct plastic pre-deformation

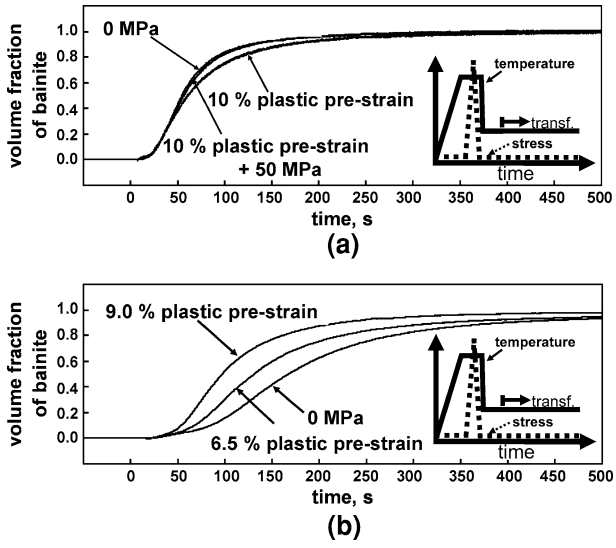

Fig. 8—Role of plastic pre-straining and additional constant external stress on the isothermal bainitic phase transformation at 340 °C. (*a*) Plastic pre-strains and external stress were applied at 880 °C following austenitization at 880 °C for 5 min (recompiled from Ref. 43). (*b*) Plastic pre-strains were applied at 1050 °C following austenitization at 1050 °C for 10 s. Samples were unloaded prior to cooling.

following the austenitization at 880 °C nor the application of an additional constant external stress of 50 MPa superimposed immediately after the pre-deformation had a significant influence on the kinetics of the isothermal phase transformation at 340 °C (Figure 8(a)). By contrast, plastic pre-deformation of the stable austenite at 1050 °C accelerated the isothermal phase transformation process (Figure 8(b)).

For both temperature-time paths transformation plasticity is prevalent when an elastic stress lower than the yield stress of the supercooled austenite is superimposed during the isothermal bainitic phase transformation (Figures 9(a) and 10(a)). Moreover, a plastic pre-deformation of the supercooled austenite also leads to pronounced transformation plasticity. Accordingly, an increase in stress or plastic pre-deformation brings about larger overall transformation plasticity (Figures 9 and 10).

Remarkably, no transformation plasticity is brought about by heavy plastic deformation of the stable austenite (Figures 9(b) and 10(b)) for both temperature-time paths (880 °C and 1050 °C). Since transformation plasticity is visible only when elastic stresses are superimposed during the phase transformation, it is assumed that the internal stress fields generated during pre-straining vanish during cooling to the isothermal phase transformation temperature of 340 °C. Thus, no driving forces remain to promote an alignment of favorable variants along the loading axis, and no transformation plasticity results.

Figure 11 displays the grain maps and the textures of two samples transformed under zero stress, where one of the samples was plastically deformed in the supercooled austenitic state to 5.5 pct strain prior to the subsequent phase transformation. The microstructure of

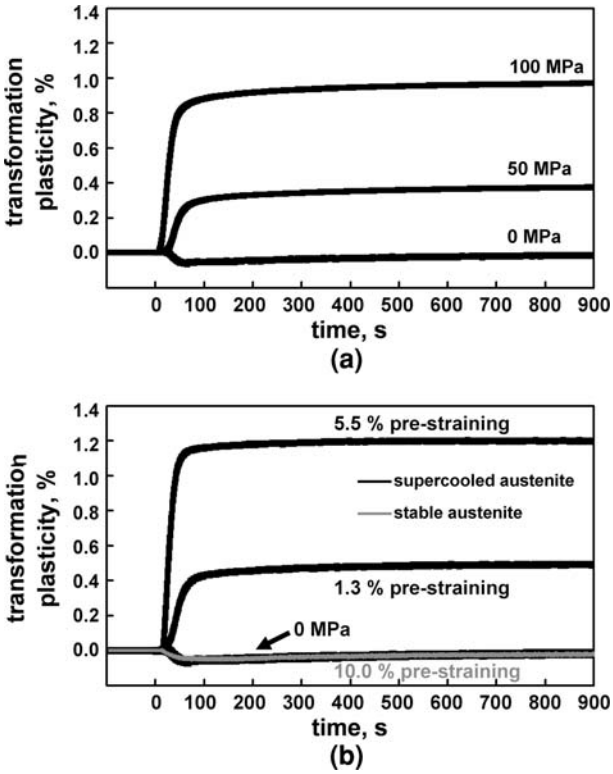

Fig. 9—Evolution of transformation plasticity during the isothermal phase transformation at 340 °C following an austenitization treatment at 880 °C for 10 s (*a*) in the presence of constant external elastic stresses and (*b*) following plastic pre-straining of stable and supercooled austenite in the absence of external stresses.

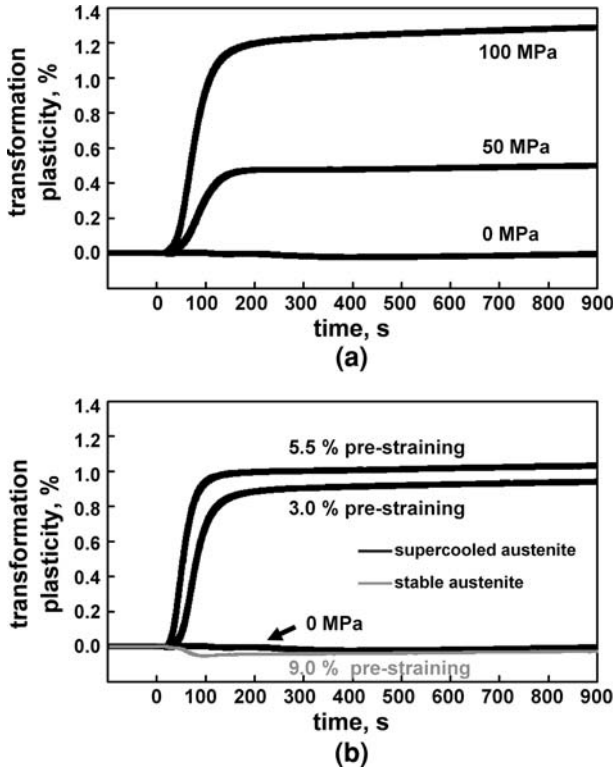

Fig. 10—Evolution of transformation plasticity during the isothermal transformation at 340 °C following an austenitization treatment at 1050 °C for 5 min (*a*) in the presence of constant external elastic stresses and (*b*) following plastic pre-straining of stable and supercooled austenite in the absence of external stresses.

the pre-deformed specimen appears slightly finer and more aligned compared to the not pre-strained one.

IV. DISCUSSION

Several reasons might explain the observed accelerated isothermal bainitic phase transformation when austenitizing took place at 880 °C for 5 minutes instead of 1050 °C for 10 seconds. For instance, diffusion of nitrogen from the surrounding environment into the samples during austenitization is one possibility. It was demonstrated in continuous cooling experiments that an increase in nitrogen content decelerates the austenite-to-ferrite phase transformation, such that the transformation start temperature decreases and the total transformation time increases concomitant with the nitrogen content.[35] The intrinsic mobility of the austenite/ferrite boundary is reduced with increasing nitrogen content, such that as the nitrogen content keeps increasing, precipitates form, further hindering the austenite-to-ferrite transformation.[35,36] In order to determine the role of nitrogen, additional experiments were performed in an argon atmosphere (Figure 2). The results demonstrate that the evolution of the bainitic volume fraction with time does not change when argon is used as the inert environment instead of nitrogen (Figure 2). Thus, in the present case, nitrogen hardening can be excluded as a possible reason for the aforementioned change in the phase transformation kinetics.

Another possible reason is a difference in the initial austenite grain size. An increase in the number of nucleation sites due to a decrease in initial austenite grain size would lead to an accelerated phase transformation[37,38] as there are more sites available for simultaneous formation of multiple variants. However, this is only the case when considering a transformation proceeding at a slow growth rate of bainite plates. When the growth rate increases a reduction in austenite grain size can as well decelerate the overall reaction rate due to the reduced volume transformed per nucleus.[37] A comparison between the two different temperature-time paths in a common temperature-time austenitization diagram reveals that the initial austenite grain sizes following the two different austenitization treatments should be almost the same.[1] Indeed, as shown in Figure 3, the initial austenite grain sizes following the two different austenitizing treatments are identical. Since there is no measurable difference in the initial austenite grain size (16 μm for both austenitization treatments), the austenite grain size can be excluded as a reason for the slower phase transformation kinetics in the samples austenitized at 1050 °C for 10 seconds.

The presence of residual carbides due to an incomplete austenitization could also be responsible for the accelerated phase transformation at 340 °C following an

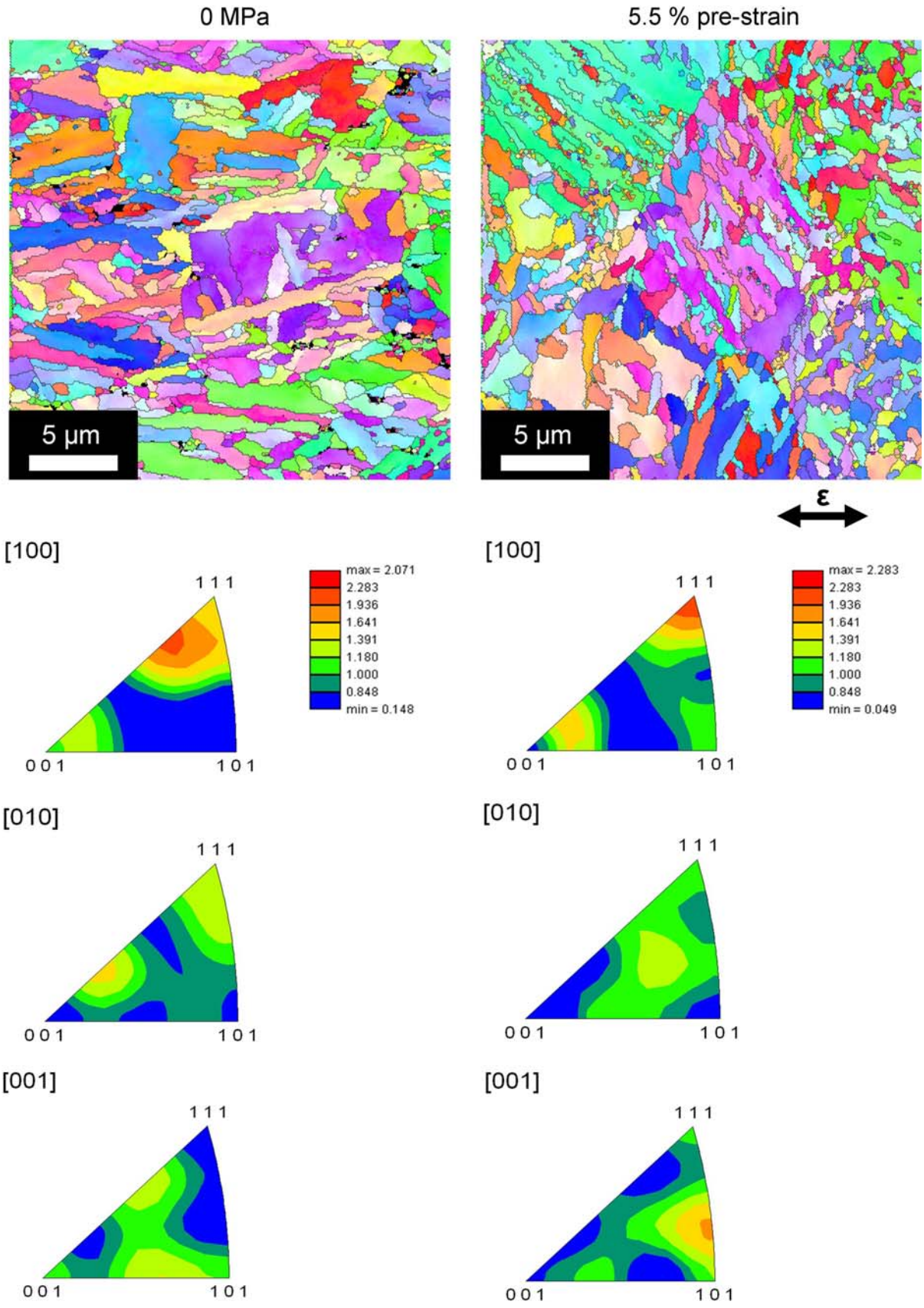

Fig. 11—Grain maps and the texture of samples austenitized for 10 s at 1050 °C and subsequently transformed isothermally to bainite at 340 °C. Axis of pre-deformation is marked with an arrow. Data were obtained through EBSD.

austenitization treatment at 880 °C for 5 minutes. Residual carbides are accompanied by a decrease of the carbon content in the matrix, which has been shown to lead to an increase in the martensite start temperature during continuous cooling experiments.[39] Specifically, a smaller amount of interstitial carbon in the matrix leads to less distortion of the martensite. Thus, the transformation, which is based on displacive transformation mechanisms, can proceed easier since less energy is needed for the martensitic transformation. When looking at the isothermal bainitic phase transformation a decrease in the carbon content of the matrix shifts the start and the end of the transition to shorter times, thus accelerating the kinetics.[1]

In addition, when local differences in the chemical composition are present due to an inhomogeneous dissolving process during austenitizing, the aforementioned acceleration effect is even reinforced since both the amount of carbon and the amount of alloying elements (*e.g.*, chromium) in the austenite matrix are reduced. Hence, less diffusion is needed during the bainitic transformation and thus the overall transformation kinetics are accelerated when the austenitizing treatment was incomplete. As shown in Figure 5 and expected from literature,[1,40] residual carbides are present when austenitizing took place at 880 °C for 5 minutes, whereas no residual carbides are visible when the steel was austenitized at 1050 °C for 10 seconds. Accordingly, the much faster phase transformation following an austenitization treatment at 880 °C as compared to the transformation following an austenitization at 1050 °C is attributed to the existence of residual carbides (Figure 5), which reduce the content of both carbon and chromium in the matrix.

The increased mechanical driving force induced by small elastic stresses superimposed during the phase transformation also accelerate the phase transformation kinetics, and the added energy supports the growth of variants along a preferred orientation with respect to the loading axis.[30,41] Since there are fewer variants in a former austenite grain as compared to the case of phase transformation without any external stresses the selected variants can grow without much resistance, which accelerates the phase transformation.[42] Small plastic strains also increase the nucleation rate of bainite plates as the density of nucleation sites is enhanced. However, as the plastic pre-deformation strains increase further, the thickness of each bainite plate will decrease since the dislocations of increasing density constitute effective obstacles on the way of the bainite phase front. Thus, heavy plastic deformation of supercooled austenite stabilizes the austenite against the bainitic reaction, such that the phase transformation is decelerated.[30] Nevertheless, this stabilization does not take place until a critical dislocation density is present, such that plastic pre-deformations with small strains still promote a faster phase transformation, as shown in Figures 6 and 7.

When pre-straining occurs at the austenitizing temperature two different observations were made. In the case of a full austenitization at 1050 °C, the increasing number of nucleation sites due to the increasing density of dislocations helps to accelerate the isothermal transformation kinetics by providing more sites available for bainite plate formation and growth, as compared to the transition under zero stress following the same austenitization treatment. On the other hand, when the austenitization treatment is incomplete (880 °C) residual carbides will constitute additional nucleation sites. However, this further increase of the number of nucleation sites does not accelerate the phase transformation process (Figure 8) as compared to a stress-free transformation following an austenitization treatment at 880 °C for 5 minutes. Indeed, formation of bainite at more locations hinders the growth since the residual carbides that remain from the incomplete austenitization as well as the already formed bainite plates act as obstacles, and thus slightly decelerates the phase transformation.[30]

It is commonly known that elastic stresses superimposed during the phase transformation can lead to transformation plasticity,[12,19,23,42] and the increase in overall transformation plasticity values is associated with a stronger alignment of the variants[27,29] or a heavier deformation of the weaker phase.[19,23,28] When variant selection yields a pronounced anisotropic volume change, a change in the final texture is also evident, which was missing in the samples of the current material that transformed under zero stress following an austenitization treatment at 1050 °C for 10 seconds (Figure 11). Similar observations were made in other studies.[8,31,44] For instance, Bate and Hutchinson argued that no strengthening of the texture takes place when the initial austenite texture is random, even in the presence of variant selection.[44] From a mathematical point of view, the strains associated with the shape change are second-order tensors. In other words, crystallographically indistinguishable orientations can have different energy products and similarly very different orientations can have the same energy product. As a result, the final texture for a crystal with cubic symmetry is expected to be close to random when the initial texture is random.[44] Nevertheless, changes in the microstructure are visible when comparing the EBSD maps of a specimen transformed under zero stress and one pre-strained. The microstructure of the specimen pre-deformed to 5.5 pct is slightly finer compared to the one of the not pre-strained sample. The availability of more nucleation sites owing to the increased dislocation density during pre-straining reduces the time necessary for the bainite plates to grow as more plates grow simultaneously.[30] Furthermore, the final microstructure of the specimen transformed without any external stresses features less grains aligned along a preferred orientation, while the pre-deformed specimen possesses many grains aligned at an angle of about 45 deg with respect to the loading axis (Figure 11). Given that the loading axis coincides with the [010] orientation, this alignment of grains can be calculated from data presented in the inverse pole figures of Figure 11. Similar behavior was observed in previous studies where the samples underwent martensitic[30,41] and bainitic[42] transformations under stress. Specifically, the preferred alignment of the grains was a result of variant selection brought about by the displacive transformation mechanism.

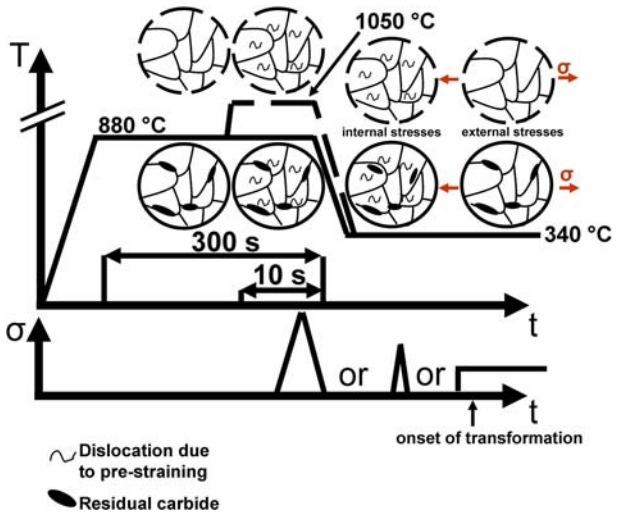

Fig. 12—Schematic illustrating the role of austenitization treatment and stress state on the microstructure of 51 CrV 4 steel. See main text for details.

The microstructural evolution of the 51 CrV 4 steel austenitized through the chosen two time-temperature paths could be summarized as follows (Figure 12). The incomplete austenitization treatment at 880 °C for 5 minutes leaves undissolved residual carbides in the matrix. This reduces the carbon content as well as the chromium content in the matrix, and in addition yields a larger number of nucleation sites for the bainite plates. Thus, the phase transformation takes place notably faster than in the case of the specimens austenitized at 1050 °C, where the austenitization is complete and no carbides are prevalent. The higher carbon and chromium content of the matrix strengthens the austenite matrix and hinders the bainitic phase transformation, such that the complete phase transformation under zero stress takes about 500 seconds longer than in the samples austenitized at 880 °C (Figure 2). For both temperature-time paths a plastic pre-deformation of the supercooled austenite, as well as application of elastic stresses lower than the yield stress of austenite superimposed during the phase transformation, accelerate the phase transformation. Dislocations introduced during the pre-straining act as additional nucleation sites,[30] and the internal stress fields surrounding the dislocations and the elastic stresses superimposed during the phase transformation provide an extra mechanical driving force further accelerating the phase transformation. Nevertheless, pre-straining of the stable austenite led to significant differences between the phase transformation behaviors of the samples austenitized at 880 °C and 1050 °C. In the first case, an already high number of nucleation sites are present due to incomplete austenitization, and thus enhanced dislocation density stemming from large pre-strains does not accelerate the phase transformation any further.

Furthermore, transformation plasticity is not evident upon pre-staining of the stable austenite, indicating that the internal stress fields vanish during cooling and the associated lack of driving forces eliminates variant selection. Similarly, the austenite deformed at 1050 °C does not feature transformation plasticity, mainly due to the lack of internal stresses. However, the increase in number of nucleation sites brought about by dislocations introduced during the pre-straining to the initially slower transforming austenite noticeably accelerates the overall isothermal phase transformation.

Overall, the current findings of the experimental study presented herein investigating the influence of both temperature and stress distribution on the overall phase transformation behavior is crucial for establishing a realistic model of the forging process, where various parameters such as temperature and stress state simultaneously govern the overall phase transformation kinetics and the evolution of the local microstructure. Thus, a deep understanding of this complicated process necessitates the knowledge of the individual roles of each governing parameter, which has been accomplished for two major factors, *i.e.*, temperature and stress distribution, in the work presented herein.

V. CONCLUSIONS

The current work was undertaken in order to investigate the role of plastic deformation and elastic stresses on the austenite-to-bainite phase transformation. Specifically, the isothermal phase transformation in a low alloy 51 CrV 4 steel was investigated, where two different time-temperature paths were used for the austenitization. Thermomechanical experiments and microscopy analyses were carried out in order to establish the influence of each parameter on the phase transformation individually, so that the basis could be established for a realistic model capable of simulating the forging process. Based on the experimental results presented herein, the following conclusions can be drawn.

1. The kinetics of an isothermal bainitic phase transformation depend strongly on the temperature-time path. An incomplete austenitization treatment at 880 °C for 5 minutes leads to a relatively faster isothermal bainitic phase transformation at 340 °C as compared to the phase transformation following an austenitization treatment at 1050 °C for 10 seconds. This acceleration of the phase transformation in the case of incomplete austenitization is attributed to the lower content of dissolved carbon and chromium in the matrix. Thus, less diffusion is needed during the bainitic transformation and the overall phase transformation kinetics are accelerated.
2. Plastic pre-deformations of the supercooled austenite, as well as elastic stresses superimposed during the phase transformation, lead to pronounced transformation plasticity. The additional energy provided by the plastic deformation or external elastic stresses promotes the growth of bainite plates along a preferred orientation and the resulting anisotropic growth brings about transformation plasticity.

3. Plastic pre-deformations of the stable austenite at 1050 °C accelerated the isothermal phase transformation at 340 °C whereas no acceleration effect was prevalent during the isothermal phase transformation upon pre-straining the stable austenite at 880 °C. Plastic pre-deformation of the former enhances the dislocation density, such that more nucleation sites become available for the formation and growth of bainite plates. In the case of pre-deformation of the austenite at 880 °C, however, there are already a large number of nucleation sites, mainly the undissolved carbides, and thus added dislocation density imposed by plastic pre-deformation does not accelerate the phase transformation any further.
4. Although the isothermal phase transformation was accelerated upon pre-straining the stable austenite at 1050 °C, no transformation plasticity was observed during the isothermal bainitic phase transformation at 340 °C. During cooling, the stress fields surrounding the dislocations diminish, such that the necessary driving force for the bainite plates to align along a preferred orientation is absent. Thus, transformation plasticity, which is facilitated by the presence of internal or external stresses, is not prevalent during the isothermal phase transformation of the samples austenitized and pre-strained at 1050 °C.

ACKNOWLEDGMENTS

Financial support by Deutsche Forschungsgemeinschaft within the Transregional Collaborative Research Centre TRR 30 ''Prozessintegrierte Herstellung funktional gradierter Strukturen auf der Grundlage thermo-mechanisch gekoppelter Phänomene'' is gratefully acknowledged. The authors also thank Mr. Juri Burow, University of Bochum, for carrying out the EBSD measurements presented herein.

APPENDIX

The austenite-to-bainite phase transition is accompanied by a characteristic volume change, which can be determined from the simultaneously measured axial (ε_a) and diametral strain (ε_d)[6]

$$\frac{\Delta V}{V} = (1+\varepsilon_a)\cdot(1+\varepsilon_d)^2 - 1 \qquad [1]$$

The volume fraction of the new phase ($w(t)$) is obtained through normalization as

$$w(t) = \frac{\Delta V}{V}(t) \Big/ \frac{\Delta V}{V}(t \to \infty) \qquad [2]$$

In addition, transformation plasticity (ε_{TP}) with respect to the loading direction can be determined as

$$\varepsilon_{TP}(t) = \varepsilon_a(t) - \frac{\Delta V}{3V}(t) = \frac{2}{3}(\varepsilon_a(t) - \varepsilon_d(t)) \qquad [3]$$

REFERENCES

1. *Atlas zur Wärmebehandlung der Stähle*, Verlag Stahleisen, Düsseldorf, 1961.
2. J. Wei, O. Kessler, M. Hunkel, F. Hoffmann, and P. Mayr: *Steel Res. Int*., 2004, vol. 75 (11), pp. 759–65.
3. U. Weidig, K. Hübner, and K. Steinhoff: *Steel Res. Int*., 2008, vol. 7 (1), pp. 59–65.
4. M. Maikranz-Valentin, U. Weidig, U. Schoof, H.-H. Becker, and K. Steinhoff: *Steel Res. Int*., 2008, vol. 79 (2), pp. 92–97.
5. L.C. Chang and H.K.D.H. Bhadeshia: *J. Mater. Sci*., 1996, vol. 31, pp. 2145–48.
6. U. Ahrens, G. Besserdich, and H.J. Maier: *HTM*, 2002, vol. 57 (2), pp. 99–105.
7. T. Antretter, F.D. Fischer, K. Tanaka, and G. Cailltaud: *Steel Res. Int*., 2002, vol. 73 (6,7), pp. 225–35.
8. A. Matsuzaki, H.K.D.H. Bhadeshia, and H. Harada: *Acta Metall. Mater*., 1994, vol. 42 (4), pp. 1081–90.
9. P.H. Shipway and H.K.D.H. Bhadeshia: *Mater. Sci. Eng. A*, 1995, vol. 201, pp. 143–49.
10. P. Ding, T. Inoue, S. Imatani, D.-Y. Ju, and E. de Vries: *Mater. Sci. Res. Int*., 2001, vol. 7 (1), pp. 19–26.
11. J. Wei, O. Kessler, M. Hunkel, F. Hoffmann, and P. Mayr: *Mater. Sci. Technol*., 2004, vol. 20, pp. 909–14.
12. J.B. Leblond, J. Devaux, and J.C. Devaux: *Int. J. Plast*., 1989, vol. 5, pp. 551–72.
13. L. Taleb and F.A. Sidoroff: *Int. J. Plast*., 2003, vol. 19, pp. 1821–42.
14. M. Wolff, M. Böhm, G. Lowisch, and A. Schmidt: *Comp. Mater. Sci*., 2005, vol. 32, pp. 604–10.
15. F. Marketz and F.D. Fischer: *Modell. Simul. Mater. Sci. Eng*., 1994, vol. 2, pp. 1017–46.
16. G. Reisner, E.A. Werner, and F.D. Fischer: *Int. J. Solids Struct*., 1998, vol. 35 (19), pp. 2457–73.
17. F.D. Fischer, G. Reisner, E. Werner, K. Tanaka, G. Cailletaud, and T. Antretter: *Int. J. Plast*., 2000, vol. 16, pp. 723–48.
18. L. Taleb and S. Petit-Grostabussiat: *J. Phys. IV*, 2002, vol. 12, pp. Pr11 187–94.
19. S. Grostabussiat, L. Taleb, J.F. Jullien, and F. Sidoroff: *J. Phys. IV*, 2001, vol. 11, pp. Pr4 173–80.
20. U. Ahrens, H.J. Maier, and A.E.L.M. Maksoud: *J. Phys. IV*, 2004, vol. 120, pp. 615–23.
21. H.J. Maier, S. Tschumak, U. Weidig, and K. Steinhoff: *Steel Res. Int*., 2008, vol. 79 (2), pp. 105–10.
22. C.C. Liu, D.-Y. Yu, K.F. Yao, Z. Liu, and X.J. Xu: *Mater. Sci. Technol*., 2001, vol. 17, pp. 1229–37.
23. L. Taleb and S. Petit: *Int. J. Plast*., 2006, vol. 22, pp. 110–30.
24. R.H. Larn and J.R. Yang: *Mater. Sci. Eng*., 2000, vol. A278, pp. 278–91.
25. P.H. Shipway and H.K.D.H. Bhadeshia: *Mater. Sci. Technol*., 1995, vol. 11, pp. 1116–28.
26. U. Ahrens, G. Besserdich, and H.J. Maier: *HTM*, 2000, vol. 55 (6), pp. 329–38.
27. C.L. Magee: Ph.D. Thesis, Carnegie Mellon University, Pittsburgh, PA, 1966.
28. G.W. Greenwood and R.H. Johnson: *Proc. R. Soc. London, Ser. A*, 1965, vol. 283 (1394), pp. 403–22.
29. S. Kundu, K. Hase, and H.K.D.H. Bhadeshia: *Proc. R. Soc. A*, 2007, vol. 463, pp. 2309–28.
30. H.K.D.H. Bhadeshia: in *Hot Workability of Steels and Light Alloys—Composites*, H.J. McQueen, E.V. Konpleva, and N.D. Ryan, eds., Canadian Institute of Mining, Minearals and Petroleum, Montreal, 1996, pp. 543–56.
31. B. Wynne, B. Hutchinson, and L. Ryde: *Scripta Mater*., 2007, vol. 57, pp. 473–76.
32. F. Frerichs, T. Lübben, F. Hoffmann, and H.-W. Zoch: *Steel Res. Int*., 2007, vol. 78 (7), pp. 560–65.
33. M. Dalgic and G. Löwisch: *Mat.-wiss. Werkstofftech*., 2006, vol. 37 (1), pp. 122–27.
34. C. Bröcker, K. Steinhoff, and A. Matzenmiller: *Comp. Meth. Mater. Sci*., 2008, vol. 8, pp. 144–53.
35. T.A. Kop, J. Sietsma, and S. van der Zwaag: *Mater. Sci. Eng*., 2002, vol. A323, pp. 403–08.
36. S.C. Baik, S.-H. Park, O. Kwon, D.-I. Kim, and K.H. Oh: *ISIJ Int*., 2006, vol. 46 (4), pp. 599 and 605.

37. A. Matuzaki and H.K.D.H. Bhadeshia: *Mater. Sci. Technol.*, 1999, vol. 15, pp. 518–22.
38. M. Umemoto, K. Horiuchi, and I. Tamuara: *Trans. ISIJ Int.*, 1982, vol. 22, pp. 854–61.
39. J. Wang, P.J. van der Wolk, and S. vand der Zwaag: *ISIJ Int.*, 1999, vol. 39 (10), pp. 1038–46.
40. H. Bungardt, H. Preisendanz, and H. Brandis: *Ber. des Vereins deutscher Eisenhüttenleute* No. 1267, Düsseldorf.
41. C.M. Wayman and H.K.D.H. Bhadeshia: in *Physical Metallurgy*, R.W. Cahn and P. Hassen, eds., Elsevier, Holland, 1996, pp. 1507–54.
42. H.K.D.H. Bhadeshia: *Bainite in Steels*, 2nd ed., Institute of Materials, London, 2001.
43. H.-G. Lambers, S. Tschumak, and H.J. Maier: *Proc. 2nd Int. Conf. on Distortion Engineering-IDE 2008*, in press.
44. P.S. Bate and W.B. Hutchinson: *J. Appl. Cryst.*, 2008, vol. 41, pp. 210–13.